Available online at www.sciencedirect.com

ScienceDirect

IFAC PapersOnline CONFERENCE PAPER ARCHIVE

IFAC PapersOnLine 53-2 (2020) 14199–14204

Closed-loop Battery Aging Management for Electric Vehicles

Gabriele Pozzato *, **Matteo Corno** *

* *Dipartimento di Elettronica, Informazione e Bioingegneria, Politecnico di Milano, Piazza L. Da Vinci 32, 20133 Milano, Italy*
e-mail: {gabriele.pozzato,matteo.corno}@polimi.it

Abstract: In this work, a closed-loop battery aging management strategy for electric vehicles is proposed. The aging management strategy, following the model predictive control rationale, optimizes aging and vehicle performance online. The proposed formulation is based on a closed-loop term which aims at tracking a user defined aging profile. A thorough simulation study validates the approach and verifies its robustness against model uncertainties and anomalous aging phenomena.

Keywords: battery aging management, electric vehicles, optimization

1. INTRODUCTION

The last decade has been characterized by an increasing interest in Electric Vehicles (EV's). However, the cost of the battery pack and uncertainties in its life expectancy still limit the widespread use of EV's. Matching the vehicle lifetime with the one of the battery is fundamental for the spread of electric mobility.

As far as electric mobility is concerned, Li-ion batteries are the preferred technology in terms of energy and power densities (Lu et al., 2013). However, Li-ion batteries are subject to aging (*i.e.*, a capacity loss). Aging phenomena can be divided in two classes: calendar and cycle aging. The former is related to capacity losses caused by the battery storage conditions.

On the other hand, cycle aging is function of the battery usage. Temperature, Depth of Discharge (DoD), and C-rate (Barré et al., 2013; Lu et al., 2013; Jaguemont et al., 2016) have been recognized as the stress factors impacting on the battery lifetime. As a matter of fact, operating the battery at high DoD, high C-rate, and high temperatures leads to an accelerated aging process.

While aging phenomena are well documented in the literature, strategies that actively employ this information are still underexplored. Hybrid vehicles have received most of the attention. As far as hybrid electric vehicles are concerned, Ebbesen et al. (2012), Serrao et al. (2011), and Pozzato et al. (2019) proposed solutions for the energy management problem based on the minimization of a cost function accounting for battery aging phenomena. The presence of multiple power sources, *e.g.*, the internal combustion engine and the battery, allows one to avoid critical operating conditions, from a battery aging standpoint, without affecting the vehicle performance. In EV's, the aging control becomes more critical because battery degradation is connected to the vehicle performance. For this reason, most of the approaches proposed in literature focus either on cell balancing (Rehman et al., 2016) or on the usage of static maps for temperature, voltage, and current (Hannan et al., 2017).

In this work, a battery aging management strategy is proposed. First, a powertrain modeling is recalled to quantify the battery capacity degradation over time. Then, the battery aging management problem is formalized as an optimal control problem. In particular, the control actions, DoD and I_{max}^{cell}, are computed minimizing an objective function accounting for both battery life and vehicle performance. Extending a previous work of the authors (Corno and Pozzato, 2019), the aging cost term is rewritten as a tracking problem of a reference aging profile. This reformulation yields a genuine closed-loop term which provides robustness with respect to anomalous aging phenomena and model uncertainties.

The paper is organized as follows. Section 2 recalls the electric vehicle model. Section 3 formalizes the battery aging management problem as an optimal control problem. Section 4 shows the capabilities of the proposed optimization architecture considering different battery aging reference profiles, unexpected aging, and model uncertainties.

2. MODELING

Considering different driving conditions, the model aims to quantify the battery aging. The main parameters of the vehicle under investigation are summarized in Table **??**.

2.1 Electric vehicle modeling

The vehicle and aging processes are modeled according to Sabatini and Corno (2018). The model considers the throttle position as an input. Given the requested power, the power absorbed or supplied by the battery is computed in a backward fashion. Therefore, the driver is modeled as a proportional regulator which aims to follow a desired speed profile v_{ref}:

$$T_m^{req} = k_p \varepsilon = k_p (v_{ref} - v) \tag{1}$$

This work was supported by MIUR SIR project RBSI14STHV.

10.1016/j.ifacol.2020.12.1051

with k_p a suitable proportional gain, v the actual vehicle speed, and T_m^{ref} the traction torque request. Given the motor torque constant k_m, the current request is computed as follows:

$$i_m^{req} = \frac{T_m^{req}}{k_m}. \tag{2}$$

(2) is saturated to I_{max}:

$$I_{max} = f(I_{max}^{cell}, \omega_m, \bar{\eta}_m) = \frac{I_{max}^{cell} V_b n_p}{\omega_m k_m} \bar{\eta}_m \tag{3}$$

where $\bar{\eta}_m$ is the average electric motor efficiency, n_p the number of cells in parallel configuration, V_b the battery pack voltage, and ω_m the motor rotational speed. I_{max}^{cell} is an output of the battery aging management strategy, which is limiting the battery cell current at the cost of increasing the battery recharge time while reducing the maximum vehicle acceleration. From now on, the capital letter I will denote quantities expressed in C-rate rather than Ampere. With i_{mot}^{sat} being the current provided by the motor, the following longitudinal dynamics is introduced:

$$M\dot{v} = i_m^{sat} \frac{k_m r_t}{R_w} - \frac{1}{2}\rho_a v^2 C_x A - F_r \tag{4}$$

with v and M the vehicle speed and mass, R_w the wheel radius, r_t the gear ratio, C_x the drag coefficient, ρ_a the air density, A the vehicle cross sectional area, and F_r the rolling resistance. The power provided by the motor for the vehicle motion is computed according to the following equation:

$$P_m = \frac{k_m i_m^{sat} v}{R_w r_t} = k_m i_m^{sat} \omega_m = T_m^{sat} \omega_m \tag{5}$$

with T_m^{sat} the motor torque. By modeling the electric machine as a static efficiency map η_m, one obtains the following expression for the battery power:

$$P_b = \begin{cases} \frac{P_m}{\eta_m(P_m)}, & \text{if } P_m \geq 0 \text{ (motor)} \\ P_m \eta_m(P_m), & \text{if } P_m < 0 \text{ (generator).} \end{cases} \tag{6}$$

If the battery pack is composed of n_{cell}, the cell power request is $P_{cell} = P_b / n_{cell}$.

Charging management. Charging events are generally determined by the state of charge and by charging stations availability, given the extremely long simulation horizon, we neglect the issue of station availability and we assume that every time the battery reaches the lower limit state of charge, the vehicle is decelerated and recharged. To control this behavior, the aging management strategy employs the DoD as a control variable. The DoD is defined to be symmetric with respect to a SoC of 50%.

2.2 Battery cell modeling

The reference Battery Management System (BMS) is equipped with a thermal management and balancing unit. Therefore, the battery pack is modeled as a single large cell with its electrical equivalent circuit and the cell current is

$$i_{cell} = \frac{v_{oc} - \sqrt{v_{oc}^2 - 4R_{cell}P_{cell}}}{2R_{cell}} \tag{7}$$

with the SoC dynamics given by:

$$\dot{SoC} = -\frac{i_{cell}}{Q} \tag{8}$$

where Q is the cell capacity, decreasing with the aging. The battery aging model, derived from Suri and Onori (2016), is given by the following set of equations:

$$\begin{cases} \frac{dQ}{dAh} = -\frac{z}{100}\alpha_{SoC} \exp\left(\frac{-E_a + \eta|I_{cell}|}{R_g(273.15+T)}\right) Ah^{z-1} \\ \dot{Ah} = \frac{1}{3600}|I_{cell}|Q_{nom} \end{cases} \tag{9}$$

with E_a and R_g the activation energy, equal to 31.5 (kJ/mol), and the universal gas constant, respectively. η and z are identified from experimental data. α_{SoC} is a penalizing factor accelerating the aging for low and high SoC:

$$\alpha_{SoC} = d\left(1 + c\, e^{b(SoC_{min} - SoC)}\right)\left(1 + c\, e^{b(SoC - SoC_{max})}\right)$$

with b, c, d, SoC_{min}, and SoC_{max} shaping parameters. Major stress factors affecting the battery lifetime modeled as in (9) are: temperature T, SoC, and C-rate I_{cell}. Eventually, the battery internal resistance variation due to temperature and aging phenomena is modeled as follows:

$$R_{cell} = R_{cell}^1 + \Delta R_{cell}. \tag{10}$$

The first term in (10) describes the resistance variation with respect to temperature (Lin et al., 2014):

$$R_{cell}^1 = R_{cell,0} e^{\left(\frac{T_1}{T - T_2}\right)} \tag{11}$$

with $R_{cell,0}$ the nominal cell resistance and T_1, T_2 identified parameters. The second term provides a linear relationship between a resistance increment ΔR_{cell} and a capacity decay ΔQ:

$$\Delta R_{cell} = -k_{res} \Delta Q \tag{12}$$

where k_{res} is derived experimentally (see, *e.g.*, Schuster et al. (2016)).

Thermal management. Cooling circuits are commonly adopted in order to control the battery pack temperature to a desired value. The introduction of such a thermal management system leads to an increment of the cell power request of P_{cool}, *i.e.*, the cooling power:

$$P_{cell}^{tot} = P_{cell} + P_{cool}. \tag{13}$$

3. BATTERY AGING MANAGEMENT

This section addresses the battery aging management issue considering as control variables I_{max}^{cell} and DoD. The goal is to control the battery aging while guaranteeing acceptable driving performance in terms of charging time, range, and drivability. We define an optimal control problem, over a traveled distance $\mathcal{N}$, as:

$$
\begin{aligned}
\underset{\mathbf{u}}{\text{minimize}} \quad & \alpha_l J_{life} + \alpha_s J_{speed} + \alpha_c J_{charge} - \alpha_r J_{range} \\
\text{subject to} \quad & \\
& (4), (8), (9) \\
& i_m^{req} = k_p(v_{ref} - v)/k_m \\
& I_{max} = f(I_{max}^{cell}, \omega_m, \bar{\eta}_m) \\
& i_m^{sat} = \begin{cases} i_m^{req}, & |i_m^{req}| \leq I_{max} Q_{nom} \\ I_{max} Q_{nom}, & i_m^{req} > I_{max} Q_{nom} \\ -I_{max} Q_{nom}, & i_m^{req} < -I_{max} Q_{nom} \end{cases} \\
& P_{cell} = P_b(i_m^{sat}, \omega_m)/n_{cell} \\
& i_{cell} = \frac{v_{oc} - \sqrt{v_{oc}^2 - 4 R_{cell} P_{cell}}}{2 R_{cell}} \\
& I_{cell} = i_{cell}/Q_{nom} \\
& \frac{1 - DoD}{2} \leq SoC \leq 1 - \frac{1 - DoD}{2}
\end{aligned}
\tag{14}
$$

where $\mathbf{u} = \left[DoD, I_{max}^{cell}\right]^T$ is the vector of control variables (with $DoD \in [20, 100]\,\%$ and $I_{max}^{cell} \in [1, 5]$ (C-rate)) and $P_b(i_m^{sat}, \omega_m)$ highlights that the battery power is computed from (5) and (6). α_l, α_s, α_c, and α_r are weighting factors which will be detailed in what follows. The minus in front of J_{range} stands for maximization.

J_{life} accounts for the tracking error with respect to a desired aging profile Q_{ref} (Figure 1):

$$
J_{life} = \sqrt{\frac{1}{t(\mathcal{N})} \int_0^{t(\mathcal{N})} \left(Q_{ref}(\tau) - Q(\tau)\right)^2 \, d\tau} \tag{15}
$$

with $t(\mathcal{N})$ the time horizon, *i.e.*, the time to travel $\mathcal{N}$ kilometers. In the program formulated by Corno and Pozzato (2019), the aging cost term is minimizing the capacity drop over $\mathcal{N}$, *i.e.*, $\frac{Q(0) - Q(\mathcal{N})}{\mathcal{N}}$. This formulation yields the control variables which guarantee the optimal battery aging in ideal conditions, *i.e.*, assuming the model (9) to be a perfect description of the real-world battery and that none of the cells are faulty. Therefore, coping with anomalous aging scenarios is not possible. Conversely, the closed-loop architecture brought by (15) enhances the robustness of the proposed aging management strategy (as will be analyzed in Section 4). J_{speed} accounts for the mismatch between the driver's desired speed v_{ref} and the actual vehicle speed v:

$$
J_{speed} = \sqrt{\frac{1}{t(\mathcal{N})} \int_0^{t(\mathcal{N})} \left(v_{ref}(\tau) - v(\tau)\right)^2 \, d\tau}. \tag{16}
$$

The terms J_{charge} and J_{range} take into account the charging time and the driving range, respectively:

$$
\begin{aligned}
J_{charge} &= \sqrt{\frac{1}{\mathcal{E}(\mathcal{N})} \sum_{i=1}^{\mathcal{E}(\mathcal{N})} t_c(i)^2} \\
J_{range} &= \sqrt{\frac{1}{\mathcal{E}(\mathcal{N})} \sum_{i=1}^{\mathcal{E}(\mathcal{N})} d_r(i)^2}
\end{aligned}
\tag{17}
$$

where $\mathcal{E}(\mathcal{N})$ is the total number of charging events over $\mathcal{N}$, t_c the charging time for each event, and d_r the traveled distance between two charging events.

The solution of the aging management problem is carried out relying on a Model Predictive Control (MPC) procedure based on Particle Swarm Optimization (PSO). Therefore, a prediction horizon $\mathcal{N}_p$ and a control discretization step $\mathcal{N}_u$ are introduced (such that $\mathcal{N}_u \leq \mathcal{N}_p$). At each MPC index k, the next $\mathrm{k_p} = \mathcal{N}_p/\mathcal{N}_u$ control moves are selected minimizing a reformulation of the objective function in (14):

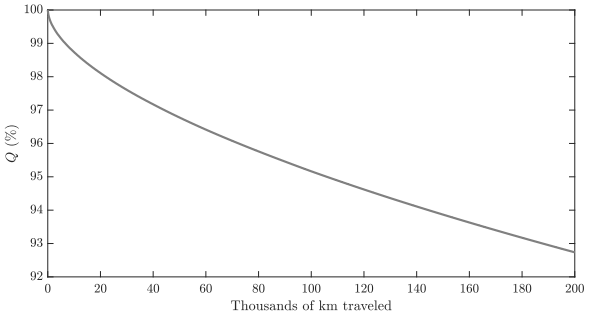

Fig. 1: Nominal battery aging reference signal. This profile is retrieved from Corno and Pozzato (2019), considering the solution for the Artemis Rural driving cycle.

$$
\begin{aligned}
J_k = \; & \alpha_l \sqrt{\frac{1}{t(k+\mathrm{k_p}) - t(k)} \int_{t(k)}^{t(k+\mathrm{k_p})} \left(Q_{ref}(\tau) - Q(\tau)\right)^2 \, d\tau} + \\
& \alpha_s \sqrt{\frac{1}{t(k+\mathrm{k_p}) - t(k)} \int_{t(k)}^{t(k+\mathrm{k_p})} \left(v_{ref}(\tau) - v(\tau)\right)^2 \, d\tau} + \\
& \alpha_c \sqrt{\frac{1}{\mathcal{E}(k+\mathrm{k_p}) - \mathcal{E}(k)} \sum_{i=\mathcal{E}(k)}^{\mathcal{E}(k+\mathrm{k_p})} t_c(i)^2} - \\
& \alpha_r \sqrt{\frac{1}{\mathcal{E}(k+\mathrm{k_p}) - \mathcal{E}(k)} \sum_{i=\mathcal{E}(k)}^{\mathcal{E}(k+\mathrm{k_p})} d_r(i)^2}
\end{aligned}
\tag{18}
$$

where $t(k+\mathrm{k_p}) - t(k)$ is the time to travel $\mathcal{N}_p$ kilometers and $\mathcal{E}(k+\mathrm{k_p}) - \mathcal{E}(k)$ the number of charging events between k and $k+\mathrm{k_p}$. Then, the receding horizon priciple is applied and only the first pair of control actions is applied from k to $k+1$. Eventually, the procedure is repeated at each k till a traveled distance $\mathcal{N}$ is reached.

In the next section, solutions of the battery aging management problem are obtained considering $\mathcal{N} = 200000$ (km), $\mathcal{N}_p = 8000$ (km), and $\mathcal{N}_u = 2000$ (km) [1]. An effective choice to solve the optimal control problem in a reasonable time, *i.e.*, 30 (min/step). Given the system state $[Q(k), SoC(k), Ah(k)]^T$ as input, prediction over $\mathcal{N}_p$ is obtained assuming perfect knowledge of the desired vehicle speed v_{ref} (Figure 3). The block diagram of the proposed online optimization strategy is summarized by Figure 2.

4. RESULTS

First, relying on a Pareto analysis, a selection of the parameter α_l is performed. Then, the proposed strategy is tested considering different aging reference signals, unexpected aging, and model uncertainties.

[1] The swarm size, a fundamental parameter for the PSO algorithm setup, is equal to 80.

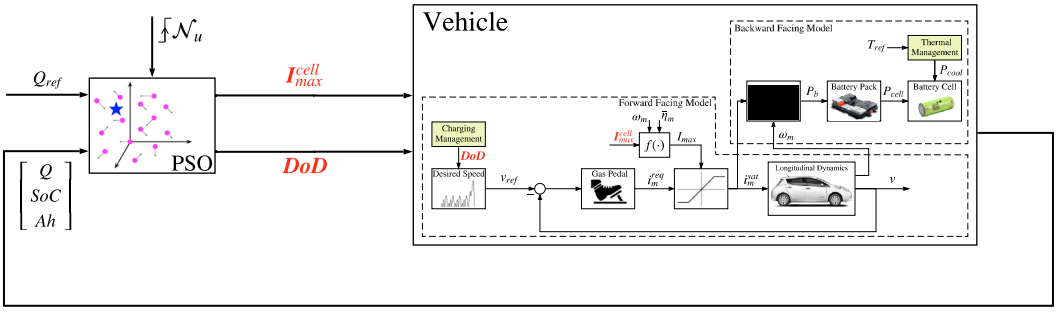

Fig. 2: Online optimization architecture. The online optimization is triggered at each control discretization step $\mathcal{N}_u$.

4.1 Pareto analysis

The objective function is a composition of four different cost terms. These components must be properly weighted in order to reach the desired performance while optimizing the system. To this end, the weighting factors for J_{speed}, J_{charge}, and J_{range} are assumed to be constant and equal to:

$$\alpha_s = 100 \text{ (s/m)}, \ \alpha_c = 1 \text{ (1/min)}, \ \alpha_r = 1 \text{ (1/km)}. \quad (19)$$

Selection of parameters (19) is performed with the goal of making the magnitude of the associated cost components comparable. Therefore, a Pareto front (see Figure 4) is constructed in order to analyze the behavior of the different cost terms while varying the parameter α_l in the range $\left[1 \times 10^4, 1 \times 10^5\right]$ (1/Ah). The higher the α_l the better the tracking of the battery aging reference profile. This is achieved at the cost of reducing both the I_{max}^{cell} and the DoD, which leads to an increased charging time and to a decreased range. Since our main goal is to track an aging profile, even in anomalous scenarios (*i.e.*, model uncertainties or unexpected aging), a value of α_l equal to 9.25×10^4 (1/Ah) is selected.

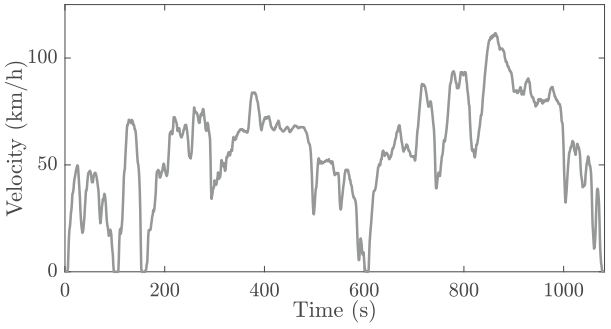

Fig. 3: The desired vehicle speed v_{ref} is modeled as an Artemis Rural driving cycle.

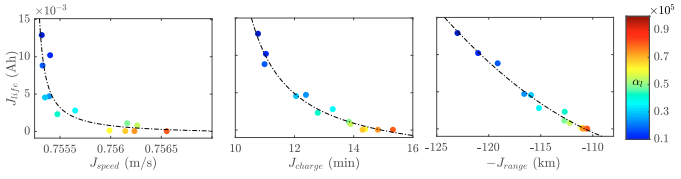

Fig. 4: Pareto analysis for α_l varying between 1×10^4 and 1×10^5 (1/Ah). The weights for J_{speed}, J_{charge}, and J_{range} are kept constant over the analysis.

4.2 Aging reference profile

To show the capabilities of the proposed approach, the battery aging management problem is solved considering different aging profiles. Starting from the nominal reference shown in Figure 1, *increased* and *decreased* aging scenarios are analyzed. As shown by Table 1, if a higher aging is allowed, both the DoD and the I_{max}^{cell} are increased, *i.e.*, an extended range (116.76 (km)) and a faster charging (12.73 (min)) are achieved. In case a lower aging is allowed, the control variables DoD and I_{max}^{cell} are reduced, leading to a range of 106.00 (km) and to a charging time of 17.88 (min). Figure 5(a) shows the tracking performance with respect to the analyzed reference profiles. Moreover, the corresponding control actions are depicted in Figure 5(b). Eventually, as shown by Table 1, the tracking performance is satisfactory and a J_{life} below 1×10^{-4} (Ah) is always guaranteed.

4.3 Robustness to unexpected aging and model uncertainties

The previous results are obtained in ideal conditions, *i.e.*, in case the battery ages according to the model (9). However, in a real-world scenario, unexpected aging phenomena, along with modeling uncertainties, may be present. Therefore, it is of paramount importance to assess the robustness of the proposed methodology even in non-ideal aging conditions.

As far as unexpected aging is concerned, a battery capacity sudden decay is introduced. This anomalous phenomenon models a fault in the battery which leads to an aging drop of 0.25% in correspondence of a traveled distance of 20000 (km). The closed-loop properties of (18) counteract this anomaly. To assess the performance of the proposed architecture, a comparison is carried out considering an open-loop scenario in which the control variables, obtained

	Nominal	**Increased aging**	**Decreased aging**
$\boldsymbol{Q}$ (%)	**92.73**	**92.31**	**92.90**
J (−)	−12.53	−24.30	47.86
J_{life} (Ah)	1.3×10^{-4}	9.1×10^{-5}	6.4×10^{-4}
J_{speed} (m/s)	0.76	0.74	0.77
J_{charge} (min)	14.39	12.73	17.88
J_{range} (km)	111.08	116.76	106.00

Table 1: Online solution for different aging reference profiles. Once the online optimization is concluded, the cost terms are computed over the entire horizon $\mathcal{N}$ as per (14).

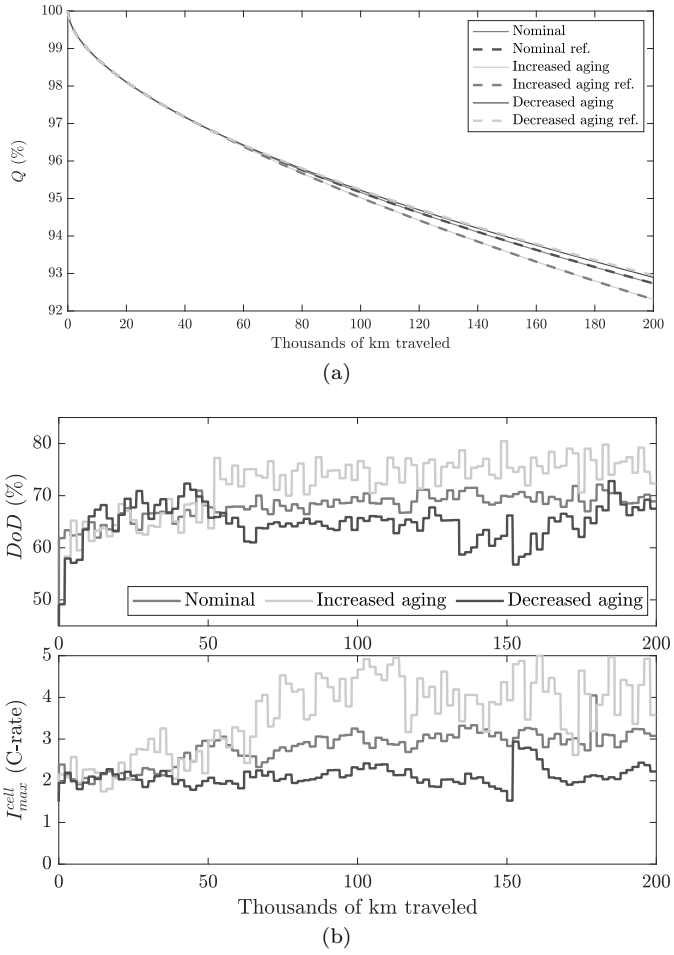

Fig. 5: Solution for different aging reference signals (a) and corresponding control actions (b). The proposed approach is effective for tracking a desired aging reference profile.

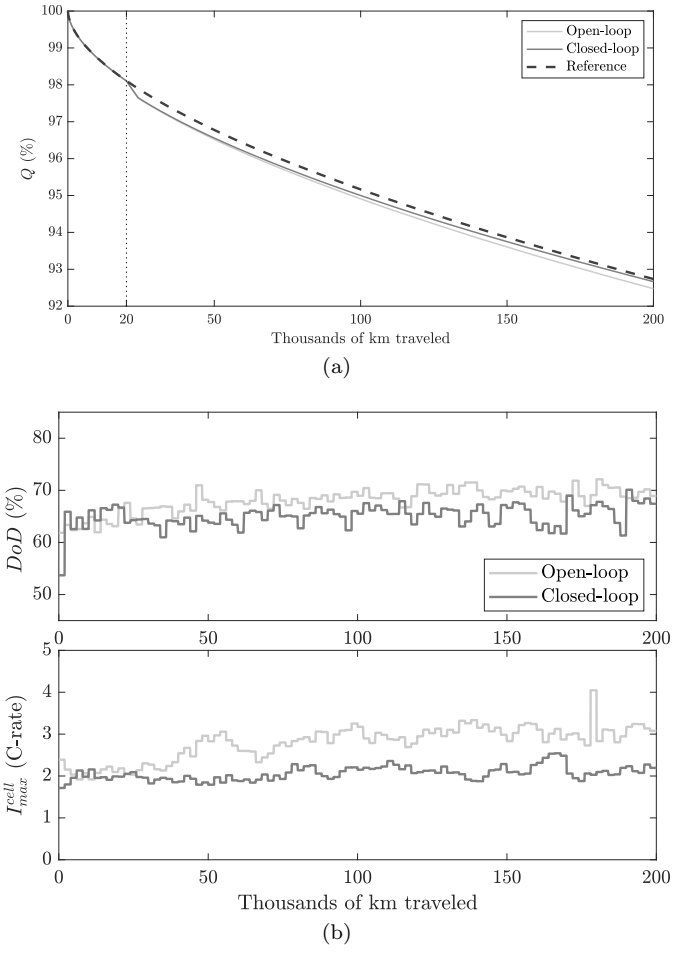

Fig. 6: Solution for the unexpected aging scenario. To assess the robustness of the proposed closed-loop strategy, the comparison is carried out with respect to an open-loop solution. (a) shows the battery aging profiles and (b) the corresponding control actions.

solving the aging management problem for the nominal aging reference profile (Figure 5(b)), are directly applied to control the system. Clearly, the open-loop approach can not recover from anomalous aging. Conversely, solving the online optimization guarantees robustness and the capability of recovering from unexpected aging limiting the performance of the vehicle, *i.e.*, reducing both the DoD and the I^{cell}_{max} (see Figure 6). Extrapolating the results to a battery end of life of 80%, the gain in terms of vehicle life extension is 14000 (km). Even though the gain is marginal, it must be noticed that the proposed methodology, for an effective choice of $\mathcal{N}_p$ and $\mathcal{N}_u$, guarantees robustness with respect to different kind (*e.g.*, harsher sudden decays) of anomalous aging scenarios. The optimization results are summarized by Table 2.

Concerning modeling uncertainties, the idea is to test the proposed online optimization architecture assuming the battery aging model used for prediction to be different with respect to the actual battery aging behavior. In practice, this is obtained modifying the parameter z in equation (9) [2]. Thus, values equal to 0.56 and 0.57 are used for the actual battery behavior and for prediction, respectively. The performance of the proposed architecture is compared to an open-loop solution, *i.e.*, the control variables obtained solving the aging management problem for the nominal aging reference profile (Figure 5(b)) are applied to control the system. Clearly, the open-loop solution can not cope with modeling uncertainties and the battery aging does not follow the user defined reference (Figure 7(a)). Conversely, the closed-loop optimization counteracts modeling uncertainties. In particular, to follow the desired aging reference and given the actual battery aging behavior, both the DoD and the I^{cell}_{max} are increased (see Figure 7(b)). Note that in this case, the change in the aging parameter leads to a longer battery life; the longer battery life comes at the cost of an underperforming vehicle. Therefore, the closed-loop solution better exploits the real capabilities of the battery pack. Optimization results are summarized by Table 3.

5. CONCLUSIONS

This paper introduces a battery aging management strategy with enhanced closed-loop properties. To this end, the aging cost term J_{life} is written as a tracking problem of Q_{ref}. Then, the optimal battery aging management is obtained minimizing an objective function composed of four terms accounting for both battery life and vehicle performance. This approach allows to track a desired ref-

[2] The parameter z strongly affects the battery aging behavior. However, uncertainty can be also present in the battery thermal model or in other parameters characterizing the aging dynamics (9).

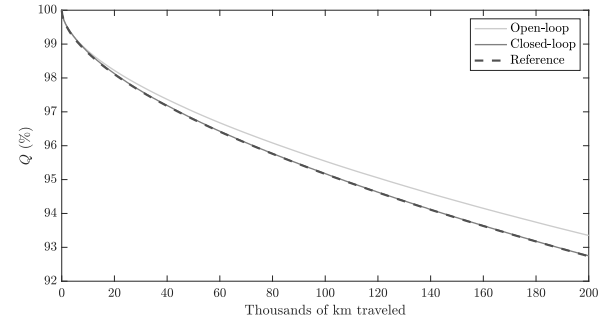

(a)

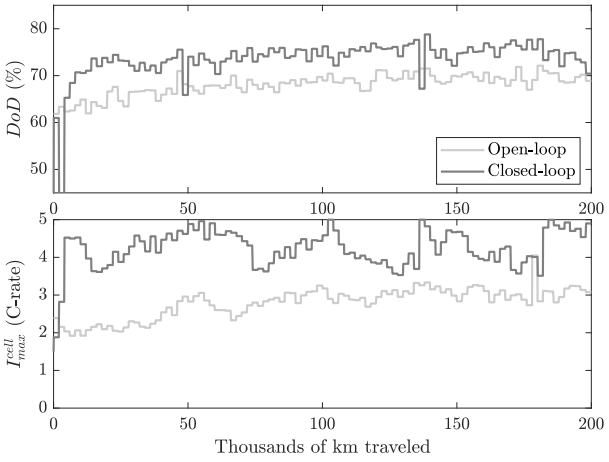

(b)

Fig. 7: Solution in case of modeling uncertainties. To assess the robustness of the proposed closed-loop strategy, the comparison is carried out with respect to an open-loop solution. (a) shows the battery aging profiles and (b) the corresponding control actions.

	Open-loop	**Closed-loop**
$\boldsymbol{Q}$ (%)	**92.48**	**92.67**
J (−)	539.61	348.60
J_{life} (Ah)	6.1×10^{-3}	3.9×10^{-3}
J_{speed} (m/s)	0.74	0.75
J_{charge} (min)	14.35	18.17
J_{range} (km)	110.37	105.86

Table 2: Online solution of the battery aging management problem for the unexpected aging scenario. Once the online optimization is concluded, the cost terms are computed over the entire horizon $\mathcal{N}$ as per (14).

erence Q_{ref} while guaranteeing a satisfactory driving experience. The proposed methodology provides robustness with respect to anomalous aging phenomena and model uncertainties.

REFERENCES

Barré, A., Deguilhem, B., Grolleau, S., Gérard, M., Suard, F., and Riu, D. (2013). A review on lithium-ion battery ageing mechanisms and estimations for automotive applications. *Journal of Power Sources*, 241, 680–689.

Cheng, K.W.E., Divakar, B., Wu, H., Ding, K., and Ho, H.F. (2011). Battery-management system (bms) and soc development for electrical vehicles. *IEEE transactions on vehicular technology*, 60(1), 76–88.

	Open-loop	**Closed-loop**
$\boldsymbol{Q}$ (%)	**93.35**	**92.75**
J (−)	885.73	−5.32
J_{life} (Ah)	0.01	3.1×10^{-4}
J_{speed} (m/s)	0.74	0.76
J_{charge} (min)	14.44	10.19
J_{range} (km)	111.16	120.04

Table 3: Online solution in case of modeling uncertainties. Once the online optimization is concluded, the cost terms are computed over the entire horizon $\mathcal{N}$ as per (14).

Corno, M. and Pozzato, G. (2019). Active adaptive battery aging management for electric vehicles. *Transaction on Vehicular Technologies*.

Ebbesen, S., Elbert, P., and Guzzella, L. (2012). Battery state-of-health perceptive energy management for hybrid electric vehicles. *IEEE Transactions on Vehicular technology*, 61(7), 2893–2900.

Hannan, M.A., Lipu, M.H., Hussain, A., and Mohamed, A. (2017). A review of lithium-ion battery state of charge estimation and management system in electric vehicle applications: Challenges and recommendations. *Renewable and Sustainable Energy Reviews*, 78, 834–854.

Jaguemont, J., Boulon, L., and Dubé, Y. (2016). A comprehensive review of lithium-ion batteries used in hybrid and electric vehicles at cold temperatures. *Applied Energy*, 164, 99–114.

Lin, X., Perez, H.E., Mohan, S., Siegel, J.B., Stefanopoulou, A.G., Ding, Y., and Castanier, M.P. (2014). A lumped-parameter electro-thermal model for cylindrical batteries. *Journal of Power Sources*, 257, 1–11.

Lu, L., Han, X., Li, J., Hua, J., and Ouyang, M. (2013). A review on the key issues for lithium-ion battery management in electric vehicles. *Journal of power sources*, 226, 272–288.

Pozzato, G., Formentin, S., Panzani, G., and Savaresi, S.M. (2019). Least costly energy management for extended-range electric vehicles with noise emissions characterization. In 9^{th} *International Symposium on Advances in Automotive Control*. IFAC.

Rehman, M.M.U., Zhang, F., Evzelman, M., Zane, R., Smith, K., and Maksimovic, D. (2016). Advanced cell-level control for extending electric vehicle battery pack lifetime. In *Energy Conversion Congress and Exposition (ECCE), 2016 IEEE*, 1–8. IEEE.

Sabatini, S. and Corno, M. (2018). Battery aging management for fully electric vehicles. In *2018 European Control Conference (ECC)*, 231–236. IEEE.

Schuster, S.F., Brand, M.J., Campestrini, C., Gleissenberger, M., and Jossen, A. (2016). Correlation between capacity and impedance of lithium-ion cells during calendar and cycle life. *Journal of Power Sources*, 305, 191–199.

Serrao, L., Onori, S., Sciarretta, A., Guezennec, Y., and Rizzoni, G. (2011). Optimal energy management of hybrid electric vehicles including battery aging. In *American Control Conference (ACC), 2011*, 2125–2130. IEEE.

Suri, G. and Onori, S. (2016). A control-oriented cycle-life model for hybrid electric vehicle lithium-ion batteries. *Energy*, 96, 644–653.